STUDY

Microscopic In Vivo Description of Cellular Architecture of Dermoscopic Pigment Network in Nevi and Melanomas

Giovanni Pellacani, MD; Anna Maria Cesinaro, MD; Caterina Longo, MD; Costantino Grana, MD; Stefania Seidenari, MD

Objective: To characterize the microscopic aspects of the dermoscopic pigment network in vivo, by means of confocal scanning laser microscopy.

Design: Confocal imaging was performed on melanocytic lesions characterized by pigment network at dermoscopy. Some confocal architectural and cytologic features, as observed at the dermoepidermal junction, were morphologically described and quantified by means of a dedicated program.

Setting: University medical department.

Study Population: We studied confocal images of 15 melanomas, 15 dermoscopic atypical nevi, and 15 common nevi.

Main Outcome Measures: Features referring to aspect, size, regularity, homogeneity, and infiltration of dermal papillae and to cellular size, regularity, and atypia were described by 2 observers on confocal images. Mean dermal papillary diameter, mean cell area, and shape irregularity were quantified by drawing papillae and cell contours on confocal images and measured with the use of a computer program.

Results: Pigment network in melanomas consisted of large basal cells that circumscribed small to medium-sized dermal papillae with marked cellular atypia, sometimes infiltrating dermal papillae. On the other hand, common acquired nevi were characterized by lack of atypical cells and edged dermal papillae. Atypical nevi presented intermediate characteristics between clearly benign and malignant lesions.

Conclusion: Cellular atypia was the most sensitive feature for melanoma diagnosis, whereas the presence of nucleated cells infiltrating dermal papillae was the most specific one.

Arch Dermatol. 2005;141:147-154

IN VIVO REFLECTANCE-MODE CONfocal scanning laser microscopy (CSLM) is a novel technique enabling the noninvasive imaging of the skin in horizontal planes at a quasi-histologic resolution.[1,2] Cellular reflectivity, shape, and distribution can be described when one attempts to characterize the physiologic or pathologic condition examined.[3-9] Because pigment melanin is a strong source of contrast in CSLM,[1] this technique seems particularly helpful for differentiating benign and malignant melanocytic lesions.[10-14] Although superficial structures such as the epidermis and papillary dermis can be visualized with high contrast, the resolution fades at depths greater than 200 µm, with a complete loss of image detail at the 250-µm depth, corresponding to the upper part of the reticular dermis.[2] Therefore, CSLM examination of flat and palpable lesions rather than nodular ones appears useful for distinguishing between atypical nevi and melanomas (MMs). Surface epiluminescence microscopy techniques such as dermoscopy enable the distinction of subsurface structures, thereby increasing diagnostic performance for MMs with respect to naked-eye examination, as confirmed by 2 meta-analysis studies.[15,16] Moreover, the correlation of dermoscopic features with histopathologic features was studied,[17-21] despite difficulties due to the different resolution and observation plane. Confocal scanning laser microscopy represents the missing link between dermoscopy and histologic examination by producing horizontal sections of the skin with precise correspondence to the dermoscopic feature at cel-

For editorial comment see page 212

Author Affiliations: Departments of Dermatology (Drs Pellacani, Longo, and Seidenari), Pathology (Dr Cesinaro), and Computer Engineering (Dr Grana), University of Modena and Reggio Emilia, Modena, Italy.
Financial Disclosure: None.

©2005 American Medical Association. All rights reserved.

Table 1. Description and Frequency of Dermoscopic Features of Pigment Network

Feature	No. (%) of Lesions		
	MMs (n = 15)	Atypical Nevi (n = 15)	Common Nevi (n = 15)
Pigment Network			
Thickness of grid line			
Delicate	1 (7)	1 (7)	14 (93)*
Broad	12 (80)	11 (73)	1 (7)*
Both	2 (13)	3 (20)	0
Size of the meshes			
Narrow	1 (7)	4 (27)	14 (93)*
Wide	12 (80)	9 (60)	1 (7)*
Both	2 (13)	2 (13)	0
Network color			
Light	2 (13)	6 (40)	13 (87)*
Dark	8 (53)	7 (47)	1 (7)
Both	5 (33)	2 (13)	1 (7)
Regularity of the network texture			
Regular	0	0	15 (100)*
Irregular	15 (100)	15 (100)	0
Homogeneity of the network structure			
Homogeneous line thickness	0	3 (20)	15 (100)
Homogeneous hole size	0	4 (27)	14 (93)
Consensus Meeting Definition†			
Typical pigment network	0	3 (20)	15 (100)*
Atypical pigment network	15 (100)	12 (80)	0

Abbreviation: MMs, melanomas.
*Significant compared with MMs ($P<.05$).
†Described in Argenziano et al.[27]

lular-level resolution and correspondence to histologic findings.

One of the most important dermoscopic criteria in the diagnosis of pigmented skin lesions is represented by the pigment network.[22-25] Alterations of network line width and hole size are frequently observed in MMs. To standardize the terminology, numerous nonreproducible network descriptors, such as regular/irregular, discrete/prominent, wide/narrow, and delicate/broad,[26] were substituted during the recent consensus meeting via the Internet[27] by the binary definition of typical/atypical pigment network, distinguishing between a uniformly spaced network with thin lines distributed more or less regularly throughout the lesion and a darkly pigmented or gray network with irregular holes and thick lines. Owing to the correlation of an atypical pigment network with a diagnosis of MM, the possibility of in vivo identification of the underlying histopathologic features would be of uppermost importance to clarify its diagnostic value and to improve diagnostic performance. The aim of our study was to identify the CSLM aspects corresponding to the pigment network and to correlate them with dermoscopic and histologic aspects.

METHODS

LESION IMAGES

This study included a total of 8328 images acquired by means of CSLM referring to melanocytic lesions, including 3097 referring to 15 MMs, 2844 referring to 15 dermoscopically atypical nevi, and 1887 referring to 15 common melanocytic nevi. All presented with the pigment network at the dermoscopic evaluation. All MMs had a Breslow thickness of less than 1 mm (mean±SD, 0.38±0.29 mm); 3 cases of these were in situ lesions. The presence of a preexisting nevus was reported in 3 of 10 MMs; 1 case showed histologic characteristics of a congenital-type nevus. Atypical nevi corresponded to lesions with equivocal aspects at clinical and dermoscopic inspection, and excision was performed to rule out an MM. Common nevi included in this study had typical dermoscopic features and were excised only for cosmetic reasons.

INSTRUMENTS

Digital dermoscopy imaging was performed with a digital videomicroscope (VideoCap 100; DS-Medica, Milan, Italy), using 20-, 50-, and 200-fold magnification and positioning the probe onto the CSLM adapter ring. The instrument has been described elsewhere.[28] The images were digitized by means of a Matrox Orion frameboard (Matrox Electronic Systems Ltd, Dorval, Quebec) and stored by an image acquisition program (VideoCap 8.09; DS-Medica) that is compatible with Microsoft Windows systems (Microsoft Corporation, Redmond, Wash). The digitized images offer a spatial resolution of 768×576 pixels and a resolution of 16 million colors.

The CSLM images were acquired by means of a near-infrared reflectance CSLM apparatus (Vivascope 1000; Lucid Inc, Rochester, NY). After acquiring the dermoscopic image, the adapter ring was filled with water and the arm of the CSLM with the ×30 water immersion objective lens (numerical aperture, 0.9) was placed onto it. The instrument and the acquisition modality for registration of single high-resolution images (475×350 µm, with a resolution of 640×480 pixels) have been described elsewhere.[2,29] An automated stepper was used to obtain a grid of 16 contiguous horizontal images at a selected depth that constructed a montage image with an 1.9×1.4-mm in vivo field of view (block image). A sequence of 30 block images was acquired for each lesion at the level of the dermal-epidermal junction and mounted by means of software we developed to obtain a 7.60×6.65-mm field of view (reconstructed image).[29]

IMAGE ACQUISITION

Before biopsy, lesion images were recorded by using digital dermoscopy and CSLM. To have an exact correspondence between dermoscopic and CSLM images, the 1-cm-diameter CSLM adapter ring was first positioned onto the skin and centered on the lesion, after which we obtained the dermoscopic and CSLM images. All lesions were then excised, after a silk suture was positioned at one pole of the specimen to clarify orientation, and the excised lesions underwent histologic examination for diagnostic confirmation and pattern correlation. Afterward, the dermoscopic image was resized and rotated for point-by-point correspondence with the reconstructed confocal image. Thus, the high-resolution confocal image could be positioned onto the x-y plane of the dermoscopic image for exact pattern correlation. Moreover, a series of equidistant histologic sections that started from the silk suture enabled the correlation of the dermoscopic and confocal aspects with histopathologic findings.

IMAGE DESCRIPTION

Dermoscopic Image Description

We used a systematic list of the traditional dermoscopic variables (**Table 1**) for description of the pigment network.[22-26] In addition, each image was classified as having either a typi-

©2005 American Medical Association. All rights reserved.

cal or an atypical pigment network according to the definition of the consensus meeting.[27]

CSLM Image Description

Together with the clinical, subjective description of the observable CSLM aspects performed by 2 observers (G.P. and S.S.), a semiautomatic method was introduced for CSLM image evaluation to obtain the quantification of architectural and cytologic features. To provide quantitative measures on manually annotated images, a computer program that is compatible with Microsoft Windows was created by using the Visual C++ 6.0 development system (Microsoft Corporation). Contours were drawn around all visible dermal papillae on reconstructed images (7.60×6.65-mm field of view) and around cells with a highly reflective cytoplasm located at basal layer on high-resolution images (475×350-μm field of view). For contouring, we used a 1-pixel–wide free-form brush without aliasing from a standard digital imaging program (Paint Shop Pro 7.0; Jasc Software Inc, Eden Prairie, Minn). Cells were chosen on the basis of visual inspection. The number of cells per lesion varied from a minimum of 20 to a maximum of 116, depending on their similarity, for a representative sample of cells per lesion. Connected areas were extracted from the background by means of a labeling algorithm. To identify regions delimited by unconnected segments, the border was progressively extended by means of the sequential application of the mathematical morphology operators dilatation and erosion with 2 different structuring elements, up to the closure of the contour.

Dermal Papillary Features

We evaluated the size and regularity of dermal papillae on the reconstructed images (7.60×6.65-mm field of view). The mean diameter of dermal papillae was computed by means of the previously described program. Moreover, we calculated the number of dermal papillae with a diameter of less than 100 μm (small papillae), those ranging from 100 to 200 μm (medium papillae), and those greater than 200 μm (large papillae). Each lesion was subsequently regarded as being characterized by small, medium, or large dermal papillae on the basis of the most frequently represented papilla category. Finally, we visually inspected dermal papillae for shape regularity (regular/irregular) and for homogeneity of aspect and distribution throughout the lesion (homogeneous/nonhomogeneous).

Cellular Aspects

According to previous reports concerning normal skin and melanocytic lesion observation by means of CSLM,[1,2,10-14] we evaluated cell size and aspect on the high-resolution images (475×350-μm field of view). We used the dedicated program to calculate mean cell area and its standard deviation (size irregularity). On the basis of cell-area values obtained from typical nevi, lesions presenting a mean cell area less than 250 μm^2 (corresponding to a mean diameter of approximately 18 μm) were regarded as being characterized by small cells, whereas large-cell lesions corresponded to higher mean cell-area measurements. Lesion cells were also morphologically described by considering cytologic atypia throughout the lesion. Three different degrees of cellular atypia were identified: *typical* was the term used for monomorphous small, polygonal cells; *mild atypia* was used when medium to large cells were round or oval, had bright cytoplasm, and had peripheral nuclei that were sporadically observable within typical cell architecture; and *marked atypia* was used when numerous cells were irregular in size, shape, and reflectivity, were round to oval or stellate, had (occasionally) branching dendritic-like structures, and were distributed throughout the lesion. Moreover, we reported the presence of nonaggregated cells inside dermal papillae by distinguishing between round to oval cells, those having refractive cytoplasm and an eccentric dark nucleus, and those having plump irregularly shaped bright cells with ill-defined borders and no visible nucleus.[10,11]

Table 2. Values Obtained by Quantitative Assessment of Dermal Papillae and Cells at the Dermoepidermal Junction

Measurement	MMs (n = 15)	Atypical Nevi (n = 15)	Common Nevi (n = 15)
Dermal Papillae			
Mean diameter, mean ± SD, μm	107.4 ± 39.7	125.5 ± 65.5	127.0 ± 54.0
Papilla type, No. (%)			
Small (<100 μm)	5 (33)	6 (40)	5 (33)
Medium (100-200 μm)	10 (67)	7 (47)	9 (60)
Large (>200 μm)	0	2 (13)	1 (7)
Cells			
Size, mean ± SD			
Area, μm^2	665.7 ± 593.5	186.8 ± 87.6*	162.8 ± 32.7*
Size irregularity	346.6 ± 186.6	81.3 ± 53.7*	63.0 ± 13.2*
Type, No. (%)			
Small	4 (27)	11 (73)*	15 (100)*
Large	11 (73)	4 (27)*	0*

Abbreviation: MMs, melanomas.
*Significant compared with MMs ($P<.05$).

Histopathologic Description

We described architectural patterns and cytologic features. Skin architecture was evaluated for regularity of the rete ridges, thinning or thickening of the epidermis, and flattening of the dermal papillae. Melanocytes were evaluated for morphologic characteristics, and the presence of papillary infiltration and melanophages was also reported.

STATISTICAL ANALYSIS

The statistical evaluation was carried out with the SPSS statistical package (release 10.0.6, 1999; SPSS Inc, Chicago, Ill). As basic statistical analysis, absolute and relative frequencies of each dermoscopic and confocal criterion were obtained, whereas mean and standard deviation were calculated for dermal papilla diameter and cell-area values. Significant differences between MMs and benign lesions were evaluated using the χ^2 test of independence (the Fisher exact test was applied if any expected cell value in the 2×2 table was <5) and the Mann-Whitney test for independent samples. A P value less than .05 was considered significant.

RESULTS

The dermoscopic aspects are summarized in Table 1, and the cytologic and architectural features that were calculated and observed in confocal images are reported in **Table 2** and **Table 3**, respectively.

COMMON NEVI

At the dermoscopic observation, common melanocytic nevi were characterized by a regular pigment network,

©2005 American Medical Association. All rights reserved.

Table 3. Description and Frequency of Confocal Microscopy Features Evaluated at Dermoepidermal Junction

Feature	No. (%) of Lesions		
	MMs (n = 15)	Atypical Nevi (n = 15)	Common Nevi (n = 15)
Dermal Papillae			
Shape			
Regular	4 (27)	2 (13)	7 (47)
Irregular	11 (73)	13 (87)	8 (53)
Aspect			
Homogeneous	1 (7)	7 (47)*	14 (93)*
Nonhomogeneous	14 (93)	8 (53)*	1 (7)*
Papillary contour			
Edged papillae	1 (7)	11 (73)*	15 (100)*
Nonedged papillae	11 (73)	4 (27)*	0*
Both	3 (20)	0	0
Cells			
Cytologic atypia			
Absent	1 (7)	9 (60)*	15 (100)*
Mild	6 (40)	6 (40)	0*
Marked	8 (53)	0*	0*
Carpet of cells	10 (67)	2 (13)*	1 (7)*
Cells in Dermal Papillae			
Nucleated	8 (53)	1 (7)*	0*
Plump bright	8 (53)	8 (53)	5 (33)

Abbreviation: MMs, melanomas.
*Significant compared with MMs ($P<.05$).

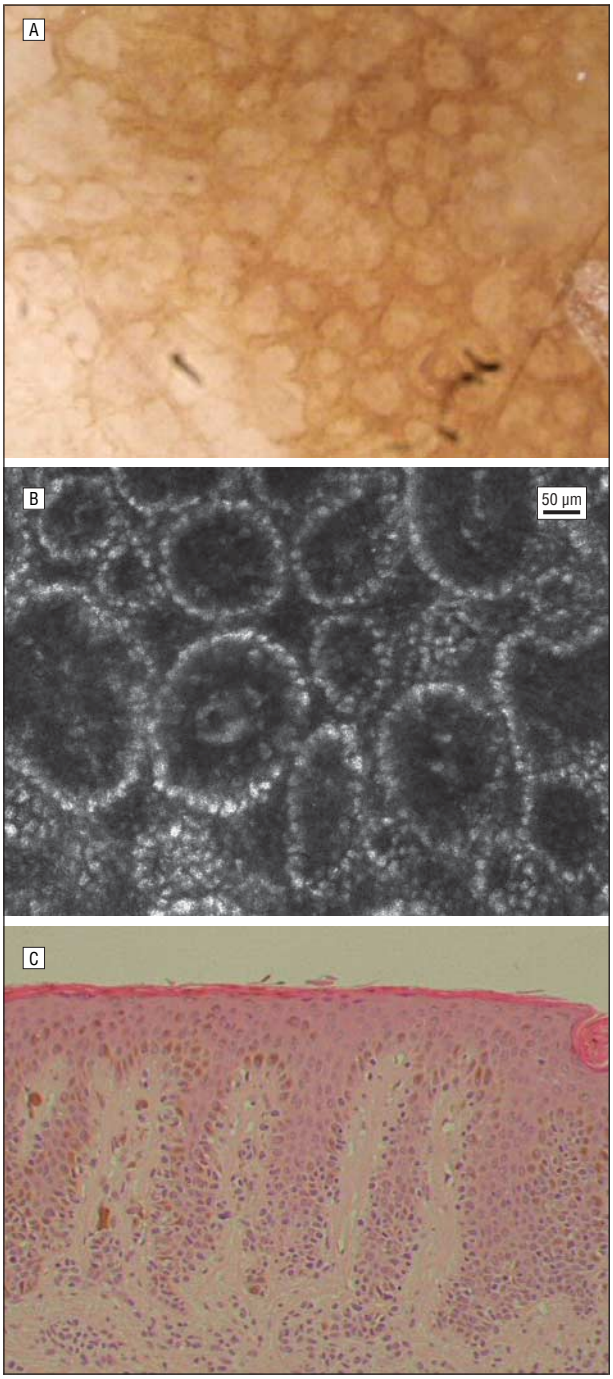

Figure 1. Pigment network in a typical nevus. A, Dermoscopic aspect characterized by a bilayer structure (original magnification ×200). B, Confocal appearance of dermal papillae edged by a rim of refractive polygonal cells without cytologic atypia (original magnification ×1000). C, Regular rete ridges and typical cytologic features at histopathologic examination (original magnification ×40).

predominantly constituted by delicate light-brown grids and narrow meshes. These lesions presented homogeneous hole size and line width. In the images obtained by CSLM, dermal papillae at the dermoepidermal junction appeared as dark round to oval areas that were medium in 9 of 15 lesions, small in 5, and large in 1, with a mean diameter of 127 µm. Dermal papillae were of regular size in 7 (47%) of the 15 lesions and were homogeneously featured in 14. In all cases, the dermal papillae were circumscribed by a rim of refractive cells that corresponded to small melanocytes and melanin-rich keratinocytes. The papillae lacked cytologic atypia and appeared as bright rings separated by a thin, structureless, slightly refractive space that sharply contrasted with the dark background (edged papillae) (**Figure 1**). In 1 lesion, with nonhomogeneous darkly pigmented areas at dermoscopy (pigment blotches), dermal papillae focally disappeared and were replaced by a stretch of bright typical cells. In that lesion, no alteration of the rete ridges and no atypical cells were observed at histologic examination. In 5 cases, some melanophages were present in the papillary dermis and correlated with the observation of plump bright cells at CSLM examination.

ATYPICAL NEVI

Atypical melanocytic nevi were predominantly characterized by an irregular pigment network that usually consisted of broad grids and wide meshes and that were darkly pigmented in 7 cases. Homogeneity of network line thickness and hole size was observed in 3 and 4 of 15 lesions, respectively. At CSLM observation, the mean diameter of dermal papillae was similar to that of common nevi. Dermal papillae were predominantly small in 6 of 15 nevi, medium in 7, and large in 2; irregular in shape in 13 cases; and nonhomogeneous in 8. In 11 of 15 atypical nevi, edged papillae were observable, whereas the remaining 4 lesions were characterized by small to medium dermal papillae without a demarcated rim of bright cells but separated by a series of large reflecting cells (nonedged

©2005 American Medical Association. All rights reserved.

papillae). In 2 cases, carpets of bright typical cells were observed. Four lesions were characterized by large cells, and 6 cases presented some medium to large cells that were round or oval, had bright cytoplasm, and had peripheral nuclei, corresponding to a mild cytologic atypia. Moreover, the presence of cells inside the dermal papilla was reported in 9 cases; in 8 of these, the cells in the dermal papilla were plump bright cells, but in 1, they were nucleated cells. At histopathologic examination, cytologic or architectural disorders were observed in most cases.

MELANOMAS

An irregularly broadened pigment network with wide, nonhomogeneous meshes characterized all MMs, except in 1 case that had an irregular, slightly pigmented, delicate grid. The dermal papillae were smaller than the nevi. Fourteen of 15 malignant lesions were formed by nonhomogeneous, small to medium dermal papillae without a demarcated rim of bright cells (nonedged papillae) (**Figure 2**) and in 3 cases with edged papillae. In a single case that corresponded to the in situ MM with a delicate pigment network at dermoscopy, edged papillae were present exclusively. Nonedged papillae, separated by a series of large bright cells, corresponded to a broadened, darkly pigmented network at dermoscopy and to a disarrangement of the dermoepidermal architecture, which was characterized by enlarged rete ridges, small dermal papillae, and epidermal flattening at histopathologic examination (Figure 2). Moreover, in 10 cases, the confocal reticular architecture, represented by lines of cells and dermal papillae, was occasionally interrupted by stretches of numerous, irregularly shaped, highly reflective cells that corresponded to pigment blotches at dermoscopy and to epidermal flattening with basal proliferation of large malignant cells at histopathologic examination. When we analyzed cytologic features by means of CSLM, MMs were characterized by larger and more irregular cells compared with acquired nevi. Marked cellular atypia was regarded as a specific marker of malignancy and was exclusively present in 8 MMs (**Figure 3**A and B). In the remaining malignant lesions, mild atypia was present (Figure 3C and D), with the exception of a single case that corresponded to an in situ MM. Large irregular cells with refractive cytoplasm and an eccentric dark nucleus infiltrating the papilla were observed in 8 of 15 MMs that had a Breslow thickness greater than 0.2 mm and that corresponded to invasive malignant cells at histopathologic examination (**Figure 4**). Moreover, plump bright cells with ill-defined borders were present in 8 of 15 MMs and corresponded to melanophages at histopathologic examination.

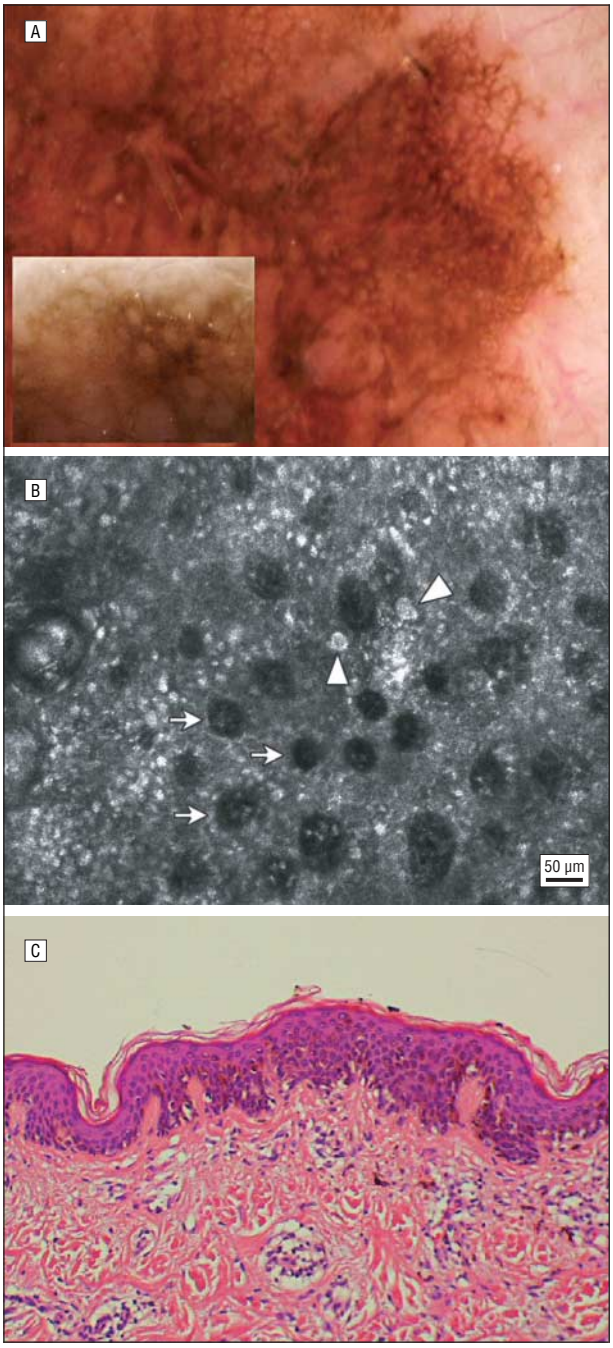

Figure 2. Atypical pigment network in an in situ melanoma. A, Dermoscopic findings of a darkly pigmented, broadened network (original magnification ×50) and a detail (inset; original magnification ×200). B, Confocal aspect shows nonedged dermal papillae (arrows) separated by a series of large, polymorphous reflecting cells (arrowheads) (original magnification ×1000). C, Histopathologic finding shows disarrangement of the dermoepidermal architecture (original magnification ×30).

COMMENT

The recent introduction of CSLM for the study of inflammatory skin disorders and skin tumors has allowed the noninvasive examination of the epidermis and superficial dermis at cellular resolution and has provided evidence of relevant correlations with histologic characteristics. For a 803-nm wavelength, melanin represents a strong source of contrast, enabling the study of melanocytic lesions with imaging depth limited to 200 to 300 µm. Thus, the study of cytologic and architectural features at the dermoepidermal junction may represent an appropriate approach for differentiating between benign and malignant melanocytic lesions. Characteristic CSLM cytologic features concerning

©2005 American Medical Association. All rights reserved.

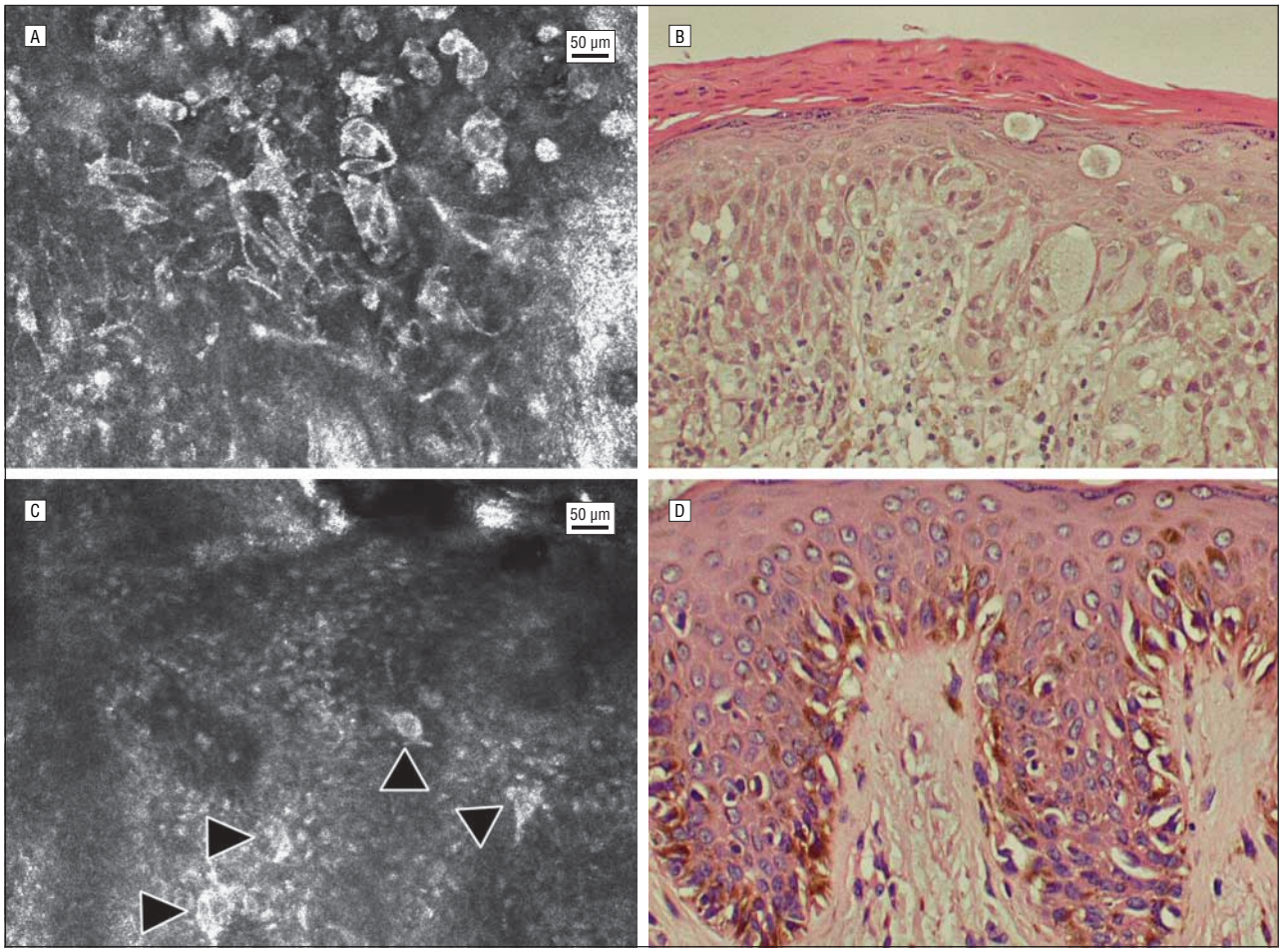

Figure 3. Cellular features. Confocal aspect (A) of marked cytologic atypia in a melanoma (original magnification ×1000), and its corresponding histologic image (B) (original magnification × 100). Confocal aspect (C) of mild cellular atypia (arrowheads) that is sporadically observable within typical cell architecture in a melanoma (original magnification ×1000), and its corresponding histologic image (D) (original magnification ×200).

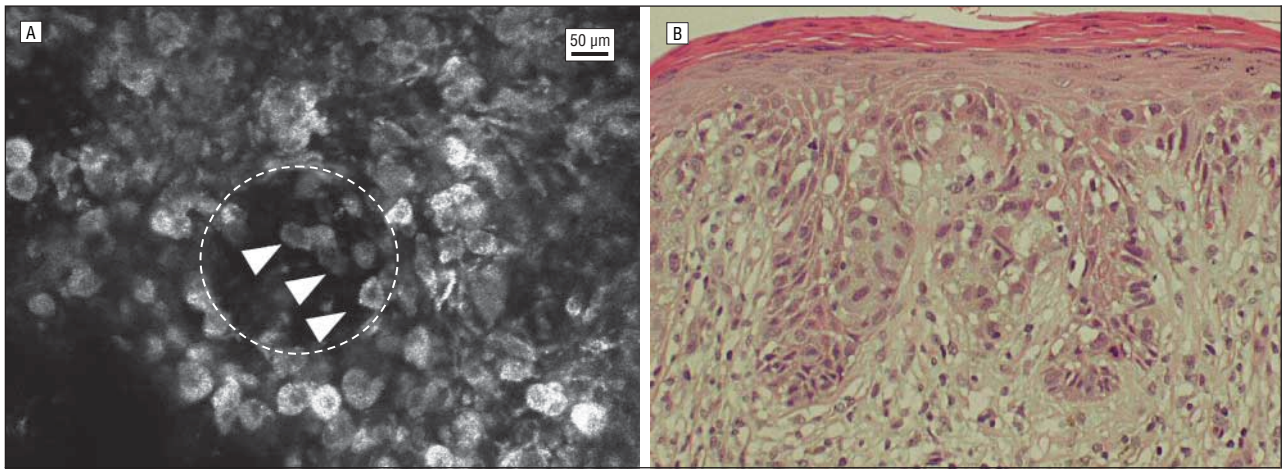

Figure 4. Confocal aspect (A) of nucleated cells (arrowheads) infiltrating dermal papilla (dashed circle) in an invasive melanoma (Breslow thickness, 0.28 mm) (original magnification × 1000), and its corresponding histologic image (B) (original magnification × 100).

melanocytic nevi and MMs have been reported, and some aspects, such as the disarray of the normal honeycombed architecture of the stratum spinosum, the presence of polymorphic reflecting cells in the basal cell layers, at times spreading upward in pagetoid fashion, and the presence of dendritic-like structures in superficial layers in lentigo maligna MMs, seem useful for MM identification.[11,13,14] Recently, we reported the possibility of an exact correlation between dermoscopic findings, CSLM features, and histopathologic findings by focusing on pigment globules as observed in Spitz nevi[29] and by characterizing different confocal features of melanocytic

©2005 American Medical Association. All rights reserved.

nests in melanocytic lesions.[30] Those studies aimed to characterize the dermal-epidermal structure by considering both cytologic features and architecture. The contemporary use of dermoscopy and CSLM image reconstruction enabled the exact identification of the dermoscopic pattern and its corresponding confocal feature. Histopathologic correlation was obtained by sectioning along an orientation line that passed through the center of the explored area. In the present study, we focused on the different confocal aspects of the dermoscopic pigment network, which is considered to be one of the most important features for differential diagnosis between melanocytic lesions.[22-25,27] Moreover, an atypical pigment network represents 1 of the 3 major criteria for MM diagnosis according to the new 7-point checklist, which is the semiquantitative algorithm based on pattern analysis proposed by Argenziano et al.[31] The CSLM evaluation enabled the characterization of cytologic and architectural aspects of the pigment network. The refractive rings circumscribing dermal papillae (edged papillae) corresponded to the darker external lines of the pigment network grids observed by means of high-magnification dermoscopy and gave rise to the bilayer network architecture previously described by Puppin and coworkers[32] (Figure 1). In contrast, small to medium dermal papillae without edge cells (nonedged papillae) correlated with a broadened dark network (Figure 2). Moreover, the characterization of cytologic features underlying specific dermoscopic aspects in melanocytic lesions enabled the identification of clues for MM diagnosis. The implementation of a quantitative method for feature description produced objective measures of characteristic confocal aspects. In our cases, MMs were characterized by large basal cells associated with small to medium dermal papillae and marked cellular atypia with large round to oval cells and/or stellate cells sometimes infiltrating dermal papillae. In our cases, the presence of cellular atypia (Figure 3) was suggestive of MM and enabled the identification of 14 of 15 malignant lesions, although 6 of 30 nevi were misclassified. Furthermore, nucleated cells infiltrating dermal papillae (Figure 4) were present in 8 of 15 MMs and in 1 atypical nevus and were considered a preliminary specific marker of malignancy. On the other hand, common acquired nevi were characterized by the lack of atypical cells and the presence of small to large edged dermal papillae that were homogeneously distributed throughout the lesion, although an irregular dermal papilla shape was present in more than half of the lesions. Atypical nevi presented intermediate characteristics between clearly benign lesions and MMs. In fact, some characteristics more frequently observable in MMs, such as the presence of nonedged nonhomogeneous papillae with large cells and cytologic atypia, were also reported in some atypical nevi.

Thus, the analysis of confocal cytologic and architectural features at the dermoepidermal junction may be of help for a more accurate distinction between MMs and acquired melanocytic nevi in the presence of dermoscopic pigment network. The implementation of a program for the composition of an overall CSLM image and the histopathologic section drawn along an established direction enabled an excellent correlation of CSLM aspects with the corresponding dermoscopic pattern and histopathologic features. In addition, CSLM allowed the in vivo characterization of the histopathologic substrate of the pigment network. Different confocal features were useful for improving MM diagnosis, although confocal features of pigment network in atypical nevi were very similar to those in MMs in some cases. Because CSLM produces horizontal planes of the skin at a quasi-histopathologic resolution, we propose the confocal study of single dermoscopic aspects and the evaluation of characteristic confocal features for the distinction between benign and malignant lesions, offering a new approach to difficult-to-diagnose melanocytic lesions to improve diagnostic accuracy in melanoma.

Accepted for Publication: June 24, 2004.
Correspondence: Giovanni Pellacani, MD, Department of Dermatology, University of Modena and Reggio Emilia, Via del Pozzo 71, 41100 Modena, Italy (pellacani.giovanni@unimo.it).

REFERENCES

1. Rajadhyaksha M, Grossman M, Esterowitz D, Webb RH, Anderson RR. In vivo confocal scanning laser microscopy of human skin: melanin provides strong contrast. *J Invest Dermatol*. 1995;104:946-952.
2. Rajadhyaksha M, Gonzalez S, Zavislan JM, Anderson RR, Webb RH. In vivo confocal scanning laser microscopy of human skin, II: advances in instrumentation and comparison with histology. *J Invest Dermatol*. 1999;113:293-303.
3. Sauermann K, Clemann S, Jaspers S, et al. Age related changes of human skin investigated with histometric measurements by confocal laser scanning microscopy in vivo. *Skin Res Technol*. 2002;8:52-56.
4. Huzaira M, Rius F, Rajadhyaksha M, Anderson RR, Gonzalez S. Topographic variations in normal skin, as viewed by in vivo reflectance confocal microscopy. *J Invest Dermatol*. 2001;116:846-852.
5. Gonzalez S, Rajadhyaksha M, Rubinstein G, Anderson RR. Characterization of psoriasis in vivo by reflectance confocal microscopy. *J Med*. 1999;30:337-356.
6. Gonzalez S, Rubinstein G, Mordovtseva V, Rajadhyaksha M, Anderson RR. In vivo abnormal keratinization in Darier-White's disease as viewed by real-time confocal imaging. *J Cutan Pathol*. 1999;26:504-508.
7. Gonzalez S, Gonzalez E, White MW, Rajadhyaksha M, Anderson RR. Allergic contact dermatitis: correlation of in vivo confocal imaging to routine histology. *J Am Acad Dermatol*. 1999;40:708-713.
8. Gonzalez S, Tannous Z. Real-time, in vivo confocal reflectance microscopy of basal cell carcinoma. *J Am Acad Dermatol*. 2002;47:869-874.
9. Hicks SP, Swindells KJ, Middelkamp-Hup MA, Sifakis MA, Gonzalez E, Gonzalez S. Confocal histopathology of irritant contact dermatitis in vivo and the impact of skin color (black vs white). *J Am Acad Dermatol*. 2003;48:727-734.
10. Busam KJ, Charles C, Lee G, Halpern AC. Morphological features of melanocytes, pigmented keratinocytes, and melanophages by in vivo confocal scanning laser microscopy. *Mod Pathol*. 2001;14:862-868.
11. Langley RG, Rajadhyaksha M, Dwyer PJ, Sober AJ, Flotte TJ, Anderson RR. Confocal scanning laser microscopy of benign and malignant melanocytic skin lesions in vivo. *J Am Acad Dermatol*. 2001;45:365-376.
12. Busam KJ, Hester K, Charles C, et al. Detection of clinically amelanotic malignant melanoma and assessment of its margins by in vivo confocal scanning laser microscopy. *Arch Dermatol*. 2001;137:923-929.
13. Busam KJ, Charles C, Lohmann CM, Marghoob A, Goldgeier M, Halpern AC. Detection of intraepidermal malignant melanoma in vivo by confocal scanning laser microscopy. *Melanoma Res*. 2002;12:349-355.
14. Tannous ZS, Mihm MC, Flotte TJ, Gonzalez S. In vivo examination of lentigo maligna and malignant melanoma in situ, lentigo maligna type by near-infrared reflectance confocal microscopy: comparison of in vivo confocal images with histologic sections. *J Am Acad Dermatol*. 2002;46:260-263.
15. Bafounta ML, Beauchet A, Aegerter P, Saiag P. Is dermoscopy (epiluminescence microscopy) useful for the diagnosis of melanoma? results of a meta-analysis using techniques adapted to the evaluation of diagnostic tests. *Arch Dermatol*. 2001;137:1343-1350.

©2005 American Medical Association. All rights reserved.

16. Kittler H, Pehamberger H, Wolff K, Binder M. Diagnostic accuracy of dermoscopy. *Lancet Oncol*. 2002;3:159-165.
17. Soyer HP, Smolle J, Hodl S, Pachernegg H, Kerl H. Surface microscopy: a new approach to the diagnosis of cutaneous pigmented tumors. *Am J Dermatopathol*. 1989;11:1-10.
18. Yadav S, Vossaert KA, Kopf AW, Silverman M, Grin-Jorgensen C. Histopathologic correlates of structures seen on dermoscopy (epiluminescence microscopy). *Am J Dermatopathol*. 1993;15:297-305.
19. Soyer HP, Kenet RO, Wolf IH, Kenet BJ, Cerroni L. Clinicopathological correlation of pigmented skin lesions using dermoscopy. *Eur J Dermatol*. 2000;10: 22-28.
20. Massi D, De Giorgi V, Carli P, Santucci M. Diagnostic significance of the blue hue in dermoscopy of melanocytic lesions: a dermoscopic-pathologic study. *Am J Dermatopathol*. 2001;23:463-469.
21. Massi D, De Giorgi V, Soyer HP. Histopathologic correlates of dermoscopic criteria. *Dermatol Clin*. 2001;19:259-268.
22. Pehamberger H, Steiner A, Wolff K. In vivo epiluminescence microscopy of pigmented skin lesions, I: pattern analysis of pigmented skin lesions. *J Am Acad Dermatol*. 1987;17:571-583.
23. Kenet RO, Kang S, Kenet BJ, Fitzpatrick TB, Sober AJ, Barnhill RL. Clinical diagnosis of pigmented lesions using digital epiluminescence microscopy: grading protocol and atlas. *Arch Dermatol*. 1993;129:157-174.
24. Pehamberger H, Binder M, Steiner A, Wolff K. In vivo epiluminescence microscopy: improvement of early diagnosis of melanoma. *J Invest Dermatol*. 1993; 100:356S-362S.
25. Steiner A, Binder M, Schemper M, Wolff K, Pehamberger H. Statistical evaluation of epiluminescence microscopy criteria for melanocytic pigmented skin lesions. *J Am Acad Dermatol*. 1993;29:581-588.
26. Stanganelli I, Burroni M, Rafanelli S, Bucchi L. Intraobserver agreement in interpretation of digital epiluminescence microscopy. *J Am Acad Dermatol*. 1995; 33:584-589.
27. Argenziano G, Soyer HP, Chimenti S, et al. Dermoscopy of pigmented skin lesions: results of a consensus meeting via the Internet. *J Am Acad Dermatol*. 2003; 48:679-693.
28. Seidenari S, Burroni M, Dell'Eva G, Pepe P, Belletti B. Computerized evaluation of pigmented skin lesion images recorded by a videomicroscope: comparison between polarizing mode observation and oil/slide mode observation. *Skin Res Technol*. 1995;1:187-191.
29. Pellacani G, Cesinaro AM, Grana C, Seidenari S. In vivo confocal scanning laser microscopy of pigmented Spitz nevi: comparison of in vivo confocal images with dermoscopy and routine histology. *J Am Acad Dermatol*. 2004;51:371-376.
30. Pellacani G, Cesinaro AM, Seidenari S. In-vivo confocal reflectance microscopy for the characterization of melanocytic nests and correlation with dermoscopy and histology. *Br J Dermatol*. In press.
31. Argenziano G, Fabbrocini G, Carli P, De Giorgi V, Sammarco E, Delfino M. Epiluminescence microscopy for the diagnosis of doubtful melanocytic skin lesions: comparison between the ABCD rule of dermatoscopy and a new 7-point checklist based on pattern analysis. *Arch Dermatol*. 1998;134:1563-1570.
32. Puppin D, Salomon D, Saurat JH. Amplified surface microscopy: preliminary evaluation of a 400-fold magnification in the surface microscopy of cutaneous melanocytic lesions. *J Am Acad Dermatol*. 1993;28:923-927.

©2005 American Medical Association. All rights reserved.